ADVANCES IN THE APPLICATIONS OF MEMBRANE-MIMETIC CHEMISTRY

Edited by
Teh Fu Yen
Richard D. Gilbert and
Janos H. Fendler

Advances in the Applications of Membrane-Mimetic Chemistry

Edited by

Teh Fu Yen
University of Southern California
Los Angeles, California

Richard D. Gilbert
North Carolina State University
Raleigh, North Carolina

and

Janos H. Fendler
Syracuse University
Syracuse, New York

Plenum Press • New York and London

Library of Congress Cataloging-in-Publication Data

On file

Based on the proceedings of an American Chemical Society Macromolecular Secretariate Symposium on Advances in Membrane–Mimetic Chemistry and Its Applications, held April 15–16, 1991, in Atlanta, Georgia

ISBN 0-306-44828-9

A Division of Plenum Publishing Corporation
233 Spring Street, New York, N. Y. 10013

Printed in the United States of America

Advances in the Applications of Membrane-Mimetic Chemistry

PREFACE

This volume had its birth from a symposium organized by the Macromolecular Secretariat of the American Chemical Society in Atlanta, GA, 1991. Since Macromolecular Secretariat has five participating divisions—Polymer Chemistry; Polymer Materials: Science and Engineering Division; Colloid and Surface Chemistry Division; Cellulose, Paper and Textile Division; and Rubber Division—the speakers were invited from these disciplinaries and they are truly interdisciplinary in multidisciplinary areas.

A number of papers are from the presentations at this symposium. However, some papers were subsequently invited to be sent in. Therefore, many papers have cited references with dates as late as this current year. This book emphasizes applications, and some of the papers were finished in 1993. Therefore, it is timely for scientists and engineers interested in this area of progress.

For scientists and engineers who are not familiar with this field, since the development is still youthful, this volume will cover some new frontiers, such as electronics, medical devices, fossil fuels, asphaltics, geochemistry, and environmental engineering. With that in mind, this book can be very useful as a reference. We do include a number of review papers in this volume. In summary, this book contains sixteen chapters with twenty-eight authors from various organizations and specialties.

We would like to take this opportunity to acknowledge the American Chemical Society for making it possible for all three editors to collaborate. The editors want to thank all the contributors for their effort in making the present volume possible. We equally appreciate their patience in waiting for this work to be completed.

Lastly, the editors would like to thank Plenum Publishing Corporation for their intent and patience. We especially would like to acknowledge Ms. Patricia M. Vann, editor, for her monumental help and thoughtful understanding, and also other copy editors of Plenum Publishing Corporation. We would like to mention Ms. Garine Gabrielian for processing the manuscripts and completing the painstaking process of checking each paper. Some parts of this book have also been checked and processed by Mr. Michael Lee and Mr. Brian Whitten, for which we are grateful.

Teh Fu Yen
University of Southern California

Richard D. Gilbert
North Carolina State University

Janos H. Fendler
Syracuse University

CONTENTS

MEMBRANE-MIMETIC APPROACH TO NANOTECHNOLOGY

Janos H. Fendler

Department of Chemistry
Syracuse University
Syracuse, New York 13244-4100

INTRODUCTION

Advanced materials in the nanometer dimension are the subject of ever increasing scrutiny, reports, and review articles.[1] Attention is increasingly focused upon the formation of "intelligent" materials which can, to different degrees, self assemble, self diagnose, self repair, and recognize and discriminate physical and/or chemical stimuli, and, at the extreme, have the capability of learning and self replicating.

Nanosized materials are size quantized; that is to say that their dimensions are comparable to the length of the de Broglie electron, the wavelengths of phonons, and the mean free paths of excitons.[2-5] Electron-hole confinement in nanosized spherical particles results in three-dimensional, quantum-size effects, i.e. in the formation of "quantum dots", "quantum crystallites", or "zero-dimensional excitons". In one-dimensional size quantization, the exciton is free to move only in two dimensions with the resultant formation of "quantum wells" or "two-dimensional excitons". In quantum wells, size quantization manifests in the growth direction, while bulk properties prevail in the other two dimensions. Finally, two-dimensional confinement of charge carriers (i.e. providing the exciton with only one-dimensional mobility) results in "quantum well wires". The importance of size and dimensionality quantizations is that they result in altered mechanical, chemical, electrical, optical, magnetic, electro-optical, and magneto-optical properties.[2-5] For example, quantum dots can be tuned by changing their diameters to absorb and emit light at desired wavelengths. This property renders the construction of finely tunable and efficient semiconductor lasers to be feasible. Semiconductor quantum dots can, in principle, be designed to capture a single electron at a time. Realization of this concept will not only provide answers to fundamental questions in quantum physics, but it will also open the door to the construction of ultrahigh density integrated circuits and information storage devices based on the presence or absence of individual electrons.[6]

The electronic structure of nanofabricated, 200-Å-diameter quantum dots was measured for the first time in 1987.[7] The method involved electron beam lithography of a chip containing a buried layer of quantum-well material, metal deposition on the

Advances in the Applications of Membrane-Mimetic Chemistry
Edited by T.F. Yen *et al.*, Plenum Press, New York, 1994

resultant surface, and the removal of the resist from and the etching away of the chip, except where it was protected by the metal layer. This and other alternative solid-state methods do not lend themselves to large scale production or to the construction of quantum dots smaller than 100 Å.

Development of a new generation of nanostructured devices requires innovative approaches which are based on a fundamental understanding of the chemistry and physics involved at the molecular level. Chemists have become increasingly involved in the various aspects of materials science. They have designed new synthetic methodologies for established materials and have created new ones with unique physical and chemical properties. Colloid chemistry is particularly well suited for advancing materials science since

- it has matured[8] and has become quantitative and predictive thanks to both the vast number of new techniques being utilized and theories being developed; and,
- significantly, many biominerals, which constitute mother nature's response to advanced materials, can be considered to be colloidal systems.

Construction of nanostructured advanced materials, based on modern "wet" colloid chemistry, has been the long-term research objective of our laboratories. Our approach has been based on membrane mimetic chemistry[9] and inspired by biomineralization.[10-15] Advantage has been taken, in this approach, of membrane mimetic systems to provide chemical and spacial control for the *in situ* generation and stabilization of ultrasmall catalytic, semiconducting and magnetic particles and particulate films. Reversed micelles,[16-22] surfactant vesicles,[23-26] bilayer lipid membranes,[27-29] Langmuir-Blodgett (LB) films,[30,31] and monolayers[32-42] have been used as membrane-mimetic systems.

SEMICONDUCTORS UNDER MONOLAYERS

We have found monolayers to be particularly useful as templates for the *in situ* generation of nanocrystalline particulate films since they mimic two-dimensional crystal growth at biological surfaces[14,15] and since precise crystallographic information has become available on the orientation and packing of surfactant headgroups from X-ray diffraction studies using synchrotron sources.[43-48] There are several advantages to using monolayer matrices for nanoparticulate film generation. First, stable, well-characterized and long-lasting monolayers can be formed from a large variety of surfactants. Second, monolayer surface areas and charges are two-dimensionally controllable and the composition of the aqueous subphase is readily variable. Third, monolayers, along with the particulate films grown under them, can be conveniently transferred to solid supports (ie. to substrates). Differences between inorganic particles generated between the headgroups of LB films[31] and particulate films formed under monolayers floating on an aqueous subphase[35-42] should be recognized. Available space between the headgroups of LB films limits the growth of the particles to 40-60 Å. Conversely, particulate films up to several thousand Å can be grown under monolayers; and, subsequent to their transfer to substrates, the surfactant monolayer can, if desired, be removed.

Experimental set-ups used for the generation and *in situ* monitoring of nanocrystalline particulate films are illustrated in Figure 1. The arrangement shown in the top allows the injection of a precursor gas (H_2S, H_2Se, NH_3, for example, while that in the bottom permits the generation of the desired gaseous precursor (Na_2S + dilute acid, for example, for generating H_2S). Facilities were available for determining surface pressure *vs.* surface area and surface potential *vs.* surface area isotherms in the

film balance placed under the glass cover. Arrangements were also made for the continuous monitoring of reflectivities; angle-dependent reflectivities; Brewster-angle and fluorescence microscopies; and non-linear optical parameters.

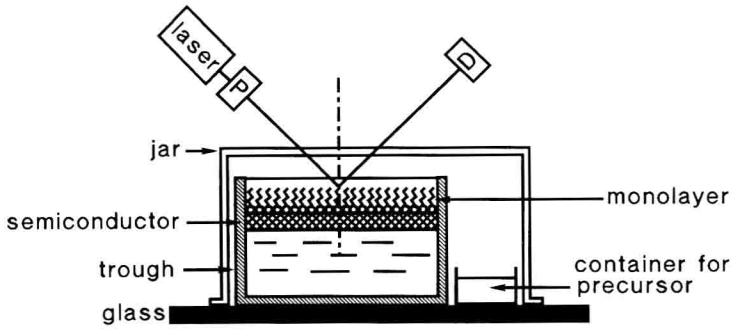

Figure 1. Schematics of the experimental arrangements used for the generation of semiconductor particles at the negatively charged, surfactant headgroup-aqueous subphase interface and that used for the in situ monitoring of reflectivities. P = polarizer and D = detector.

Evolution of a nanocrystalline particulate film, illustrated by the formation of sulfide semiconductor particulate films (Figure 2), has been discussed in terms of the following steps:[35]

a) formation of metal-sulfide bonds at a large number of sites at the monolayer-aqueous interface;
b) downward growth of well-separated nanocrystalline metal sulfide particles;
c) coalescence of clusters into interconnected arrays of semiconductor particles;
d) formation of the "first layer" of a porous sulfide semiconductor particulate film composed of 20- to 40-Å-thick, 30- to 80-Å-diameter particles;
e) diffusion of fresh metal ions to the monolayer head group area;
f) formation of a "second layer" of the porous sulfide semiconductor particulate film (by using steps a, b, and c); and
g) build-up of "subsequent layers" of the sulfide semiconductor particulate film (by using steps a, b, and c) up to a plateau thickness (ca. 300 Å for CdS and ca. 3500 Å for ZnS) beyond which the film cannot grow.

The presence of a monolayer with an appropriate surface charge is an essential prerequisite for sulfide semiconductor particulate film formation. Infusion of H_2S over an aqueous metal-ion solution, in the absence of a monolayer, resulted in the formation of large, irregular, and polydispersed metal-sulfide particles which precipitated in the bulk solution before settling to the bottom of the trough. Furthermore, no sulfide semiconductor particulate film formation could be observed

upon the infusion of H_2S to a positively charged monolayer (dioctadecyldimethylammonium bromide, for example) floating on an aqueous metal-ion ($CdCl_2$, for example) subphase.

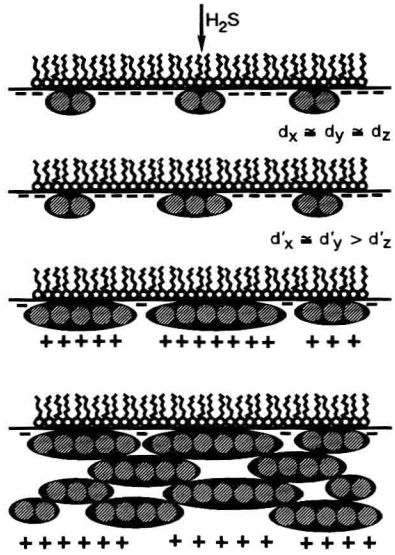

Figure 2. Proposed schematics for the initial and subsequent growth of a monolayer-supported, porous, SQSPF. The d_x and d_y dimensions are in the plane and the d_z dimension is normal to the plane; they refer to the earliest observable particles. d'_x, d'_y, and d'_z are dimensions in the plane and are normal to the plane; they refer to particles observed at later stages of their growth.

To-date, cadmium sulfide, zinc sulfide, lead sulfide, cadmium selenide, and lead selenide semiconductor particulate films have been grown, in situ, under monolayers.[33,35-42,49] Absorbances (A) increased linearly with increasing thicknesses of the CdS and ZnS particulate films. Absorption coefficients, σ-values, were calculated from

$$\sigma = A/d'_s \qquad (1)$$

and determined to be 2.4×10^5 cm^{-1} at 239 nm and 5.8×10^4 cm^{-1} at 475 nm for the CdS particulate film. These values agreed well with that determined for electrodeposited CdS films (σ (435 nm) = 2.06×10^4 cm^{-1}). Similarly, an absorption coefficient of 5.8×10^4 cm^{-1} at 315 nm was determined for the ZnS particulate film. Knowledge of absorption coefficients facilitated the assessment of direct band-gap energies, E_g, from

$$(\sigma h\omega)^2 = (h\omega - E_g)C \quad (2)$$

where $h\omega$ is the photon energy. Typical plots of the data, as determined by Eq. 2, are shown in Figure 3.[36] Values of E_g for CdS particulate films of d'_s = 63 Å, 125 Å, 163 Å, 204 Å, and 298 Å were assessed to be 2.54 eV, 2.48 eV, 2.46 eV, 2.44 eV, and 2.43 eV (Figure 3). Henglein's published E_g vs. particle-size curve[2] was used to estimate the average diameter of the 63-Å-thick CdS particles to be ca. 50 Å.

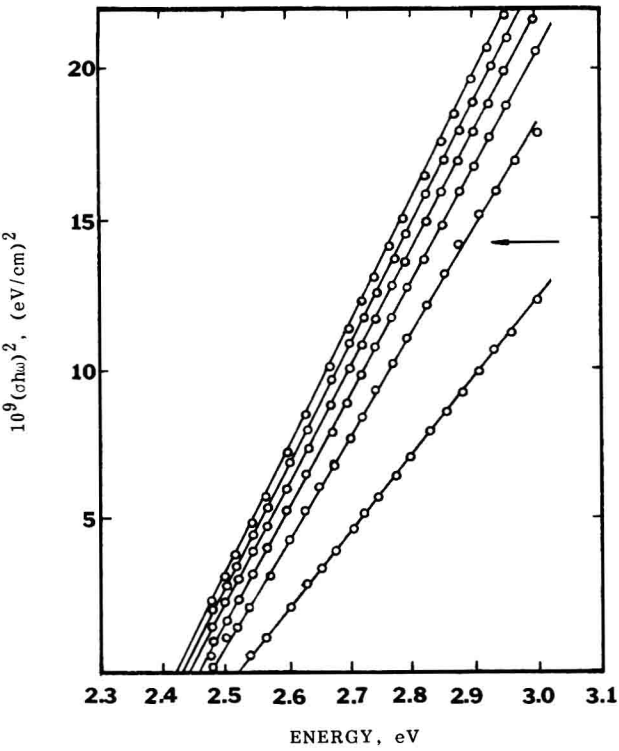

Figure 3. Plots of $(\sigma h\omega)^2$ against energy for 63-Å-, 125-Å-, 163-Å-, 204-Å-, 263-Å-, and 298-Å-thick (in the order shown by the arrow) CdS particulate films.

Increasing the thickness of the CdS particulate film resulted in progressively decreased direct band-gaps and, hence, in progressively larger CdS particles. The thickest CdS particulate film studied exhibited a direct band-gap equal to that reported for bulk CdS semiconductors (2.4 eV).[2] A direct band-gap of 3.75 eV was assessed for the 359-Å-thick ZnS particulate film.

Prolonged heating of the semiconductor particulate films at high temperatures resulted in pronounced changes in their absorption spectra. The absorbance of a 192-Å-thick CdS particulate film (vacuum dried at 10^{-3} torr for three days) decreased upon heating at 490° C for 5, 15, and 25 minutes.[36,37,49] Five minutes of heating shifted the direct band-gap from 2.47 eV to 2.40 eV (or to an absorption edge of 515 nm) equal to that of bulk CdS. A similar behavior was noted for 359-Å-thick ZnS particulate films; heating at 300° C for 15 minutes shifted the direct band-gap from 3.75 eV to 3.64 eV (or to an absorption edge of 340 nm). Prolonged heating of semiconductor particulate films have, therefore, two important consequences. First, their properties become similar to those found for bulk semiconductors. Second, they are annealed to the substrate. Annealed semiconductor particulate films could not be washed or wiped away from their substrates. In contrast, vertical dipping of untreated semiconductor particulate films into water resulted in a partial loss of material from the subphase. Interestingly, annealing of semiconductor particulate films, prepared under thiol surfactants, resulted in band-gap shifts to higher energy.[50] Transmission electron micrographs of 30- to 50-Å-thick CdS particulate films indicated the presence of 20- to 80-Å-diameter particles possessing a relatively narrow size distribution and average diameters of 47 Å.[34,36] HOPG was established, using scanning tunneling microscopy (STM), to provide an atomically flat surface with periodic roughnesses in the order of 1 Å. In two-dimensional STM images of HOPG-supported ZnS and CdS particulate films, the presence of 10- to 20-Å-thick, 30- to 40-Å-diameter ZnS and 20- to 30-Å-thick, 40- to 50-Å-diameter CdS particles is clearly discernable. The widths of the semiconductor particles observed by STM agree well with the corresponding diameters determined by transmission electron microscopy.[34,36]

Electrical and photoelectrical measurements were carried out on CdS particulate films deposited on glass substrates or teflon sheets.[36] The resistivity (ρ) of a semiconductor particulate film, measured between two parallel copper electrodes, is given by

$$\rho = R \frac{Ld'_s}{a} \tag{3}$$

where R is the measured resistivity in Ω, L is the length of the copper electrodes, a is the distance between them, and d'_s is the thickness of the semiconductor particulate film. Resistivities of 200- to 300-Å-thick CdS particulate films were determined to fall in the range of $(3\text{-}6)10^7$ Ω cm. These values represent the measurement of 10 samples of different thicknesses and may be attributed, in part, to the presence of different amounts of water in the films. The ρ values determined for CdS particulate films are some six orders of magnitude higher than those observed for materials having intrinsic conductivity.

The dark resistance of CdS particulate films was found to decrease exponentially with increasing temperature.[36] Illumination decreased the resistivity (i.e. increased the conductivity) of CdS particulate films by some two orders of magnitude and matched the absorption spectrum of the corresponding CdS particulate film nicely. Photoconductivity originates, therefore, in the production of conduction band electrons, e^-_{CB}, and valence band holes, h^+_{VB}, during band-gap irradiation of CdS:

$$CdS \xrightarrow{h\nu} e^-_{CB} + h^+_{VB} \tag{4}$$

Steady-state irradiation of CdS particulate films also resulted in the development of photovoltage. Irradiation by a 10-nsec, 343-nm laser pulse gave rise to a transient photovoltage. The magnitude of the photovoltage (1-8 mV) was found to increase linearly with the energy of the laser pulse (0.1-1.0 mJ). The rise time of the transient signal, corresponding to Eq. 4, was faster than the response time of the instrument used (10 nsec). The decay time of the signal was on the order of 3×10^{-4} seconds. This decay corresponds to charge recombination.

ORIENTED PARTICULATE GROWTH UNDER MONOLAYERS: MOLECULAR RECOGNITION

Molecular recognition between the monolayer headgroups and incipient semiconductor nanocrystallites can, in many ways, be regarded as mimicking biomineralization[10-13] and represents an important milestone in the realization of the potential of a colloid-chemical approach to band-gap engineering. Lead sulfide (PbS) particulate films composed of highly oriented, equilateral-triangular crystals have been in situ generated by the exposure of AA-monolayer-coated, aqueous, lead-nitrate [$Pb(NO_3)_2$] solutions to H_2S (Figure 4).[41] AA monolayers, in their solid states, consist of $CH_3(CH_2)_{18}COOH$ molecules two-dimensionally arrayed at the air-water interface. Spread over the aqueous subphase, the carboxyl or the carboxylate groups of AA are aligned perpendicularly to the water surface. The alkyl chains of AA, fully extended in the air in a planar zig-zag conformation, are oriented approximately normal to the surface in a triangular lattice of hexagonal close packing with a lattice constant of a = 4.85 Å.[44,51] Combined synchrotron X-ray reflection and diffraction data established a structural model for AA monolayers at air-water interfaces. The model required the hydrocarbon chains to be well packed in a pseudohexagonal lattice and tilted toward their nearest neighbor.[52]

Rationalization of the packing of the AA headgroups at the water-air interface is, unfortunately, less than straightforward.[45] The absence of information concerning the extent of headgroup ionization (at a bulk pH of 5.5), counterion binding, and the degree of hydration hinders the interpretation of experimental results and the development of a reliable theoretical approach for predicting headgroup organization at the monolayer-subphase interface. Using the experimentally determined value for the surface area of one AA molecule (20.0 $Å^2$/molecule) permitted assessment of the lattice constant to be 4.81 Å (a) and the $d_{(100)}$ spacing to be 4.16 Å ($d_{(100)} = a \cdot \sin 60°$). These values are in good agreement with those determined for AA monolayers by synchrotron X-ray scattering (a = 4.85 Å and d_{100} = 4.13 Å).[44] They are also similar to those determined for cadmium stearate (a = 4.89 Å and $d_{(100)} = 4.20 \pm 0.10$ Å) and other fatty acid monolayers.[44,51]

Reliable assessment of the arrangement and crystallinity of AA-monolayers supported by a Pb^{2+} subphase is equally elusive. Our data is best accommodated in terms of an AA:Pb^{2+} = 3:4 ratio (Figure 5). Grazing incidence X-ray diffraction measurements of lead arachidate monolayers demonstrated the existence of long-range ordering (250 Å) of Pb^{2+}.[51]

PbS is known to crystallize in a cubic crystalline lattice with a lattice constant of a = 5.9458 Å. Atomic coordinates are (0,0,0) and (½,½,0) for Pb and (½,½,½) and (0,0,½) for S. The nearest-neighbor separation of Pb-Pb and S-S atoms of 4.20 Å matches the $d_{(100)}$ network spacing of the AA monolayer. This fit implies the alignment of PbS along its (111) plane to the (100) plane of the AA monolayer (Figure